ORIGINAL RESEARCH

High Intensity Focused Ultrasound (20 MHz) and Cryotherapy as Therapeutic Options for Granuloma Annulare and Other Inflammatory Skin Conditions

Jacek Calik · Tomasz Zawada · Natalia Sauer · Torsten Bove

ABSTRACT

Introduction: In dermatology, inflammatory skin conditions impose a substantial burden worldwide, with existing therapies showing limited efficacy and side effects. This report aims to compare a novel immunological activation induced by hyperthermic 20 MHz high intensity focused ultrasound (HIFU) with conventional cryotherapy. The bioeffects from the two methods are initially investigated by numerical models, and subsequently compared to clinical observations after treatment of a patient with the inflammatory disease granuloma annulare (GA).

Methods: Clinical responses to moderate energy HIFU and cryotherapy were analysed using numerical models. HIFU-induced pressure and heat transfer were calculated, and a three-layer finite element model simulated temperature distribution and necrotic volume in the skin. Model output was compared to 22 lesions treated with HIFU and 10 with cryotherapy in a patient with GA.

Results: Cryotherapy produced a necrotic volume of 138.5 mm^3 at -92.7 °C. HIFU at 0.3–0.6 J/exposure and focal depths of 0.8 or 1.3 mm generated necrotic volumes up to only 15.99 mm^3 at temperatures of 68.3–81.2 °C. HIFU achieved full or partial resolution in all treated areas, confirming its hyperthermic immunological activation effect, while cryotherapy also resolved lesions but led to scarring and dyspigmentation.

Conclusion: Hyperthermic immunological activation of 20 MHz HIFU shows promise for treating inflammatory skin conditions as exemplified by GA. Numerical models demonstrate minimal skin necrosis compared to cryotherapy. Suggested optimal HIFU parameters are 1.3 mm focal depth, 0.4–0.5 J/exposure, 1 mm spacing, and 1 mm margin. Further studies on GA and other inflammatory diseases are recommended.

J. Calik · N. Sauer
Old Town Clinic, Wszystkich Świętych 2a, 50-127 Wrocław, Poland

J. Calik
Department of Clinical Oncology, Wroclaw Medical University, 50-556 Wrocław, Poland

T. Zawada (✉) · T. Bove
TOOsonix A/S, Agern Allé 1, 2970 Hoersholm, Denmark
e-mail: tomasz.zawada@toosonix.com

N. Sauer
Faculty of Pharmacy, Wroclaw Medical University, 50-556 Wrocław, Poland

<div style="border: 1px solid #ccc; padding: 10px;">

Key Summary Points

Why carry out this study?

Inflammatory skin conditions present a significant burden and affect millions worldwide as existing pharmacological and device-based therapies often have poor efficacy and unwanted side effects.

This report aims to understand the bioeffects of moderately dosed 20 MHz high intensity focused ultrasound (HIFU) on the upper layer of human skin, and compare it to cryotherapy commonly used in dermatology, as preclinical studies suggest that HIFU can induce immunogenic cell death and immune sensitization, potentially leading to generalized lesion regression and thereby a new modality for treatment of inflammatory skin conditions.

What was learned from the study?

The numerical modelling analysis shows that the moderate levels of HIFU can accurately target the upper dermis, creating extremely localized necrotic volumes several times smaller than those generated by conventional liquid nitrogen cryotherapy.

Clinical results from a single patient with the inflammatory skin disease granuloma annulare (GA) confirm the efficacy of HIFU treatment, showing full or partial recovery with reduced scarring and dyspigmentation compared to cryotherapy.

The study concludes that HIFU treatment slightly below the threshold for ablative response presents significant advantages over cryotherapy for treating inflammatory skin conditions, including reduced scarring and dyspigmentation.

</div>

INTRODUCTION

Inflammatory skin conditions present a significant burden and affect millions worldwide. Traditional standard of care typically includes pharmaceutical-based therapy, such as corticosteroids or imiquimod, or device-based therapies, typically by use cryotherapy or various light therapies. Both pathways, however, have significant side effects and relatively low efficacy [1]. Alternative therapeutic interventions are therefore needed.

Within the field of dermatology, 20 MHz high intensity focused ultrasound (HIFU) has recently been demonstrated as a safe and efficient device-based therapy for medical indications such as basal cell carcinoma (BCC), Kaposi sarcoma and cutaneous neurofibroma and more aesthetic conditions including seborrheic keratosis and angiomas [2–4]. These therapies primarily rely on lesion destruction by cell necrosis and tissue denaturation. The biological response to treatment is active transport of damaged cells and tissue, either to an external wound crust or internally through the vascular and lymphatic systems. By nature, these methods can thus be characterized as directly or indirectly ablative.

Results of preclinical studies on murine models with HIFU suggest that local ablative techniques can induce immunogenic cell death (ICD), increased tumour infiltration by macrophages, as well as CD4+ and CD8+ lymphocytes [5]. Therefore, HIFU can also effectively induce immune sensitization, which can contribute to more generalized lesion regression without full ablation of the lesion field [5–7].

This latter modality inducing various paths of immunological activation by HIFU dosed at more moderate energy levels than in the previous ablative treatments therefore presents an intriguing option for development of new interventional therapies for the large range of inflammatory skin conditions present in daily dermatological practice.

As a first step in understanding this new approach, this paper sets out to calculate the clinical effects of a relatively gentle hyperthermia and immunological activation induced by HIFU. These effects are compared to cryotherapy as one of the most common device-based therapies for inflammatory skin diseases.

This is initially done by creating a three-layer numerical skin model [8, 9] in combination with finite element modelling (FEM) [10–12] to evaluate clinically relevant bioeffects of treatment.

The approach allows for a unified analysis as the FEM allows for simulation of multi-physics interaction of tissue with several different energy fields, including the acoustic and thermal fields represented by the two treatment modalities. The same set of material parameters characterizing the relevant superficial tissue layers are uniformly used throughout all analyses. The impact on the skin tissue is quantified by a calculation of induced necrotic dose volume depending on the treatment exposure parameters [13, 14]. A concept of equivalent dose is introduced that allows for direct comparison of the total impact on the skin tissue of the modalities as well as other parameters such as the total time of treatment.

The model findings are used to compare and discuss a clinical case of treatment case of granuloma annulare (GA). GA is a rare, chronic inflammatory disease with an estimated incidence of approximately 1 in 10,000, accounting for less than 1% of all skin disorders [15]. The etiology of annular granuloma is not well understood [16]. It predominantly affects individuals between the ages of 20 and 40 years and is more common in women [15, 17]. GA has been described in patients of various races and ethnicities, with no evidence suggesting a specific race is more predisposed than others [18]. One theory regarding the cause of granuloma annulare is an immunological disturbance that leads to the activation of the immune system, resulting in increased cytokine production and infiltration of inflammatory cells in the skin [19, 20]. Studies have shown the presence of T lymphocytes, dendritic cells, and other inflammatory cells in the affected skin areas, indicating a probable immunological reaction associated with the disease.

The most common manifestation of GA is the appearance of single or multiple-ringed, erythematous plaques [17]. The lesions can range in colour from pink, red, and brown to purplish. The disease primarily affects the extremities (hands, feet, wrists) but can also occur on the neck and trunk [20]. Although GA is considered a benign condition, complications can arise from both treatment interventions and the natural course of the disease. Common complications include the formation of scars in previously affected areas. Secondary infections are also possible as the damaged skin caused by GA may increase the risk of bacterial or fungal infections. Conventional treatment modalities, such as topical and systemic steroids, have been used with varying degrees of success [17, 21–24]. However, these drug-based therapies have several limitations, including inadequate responses, relapse, and side effects.

GA is characterized by a low cure rate, with only 46.6% of cases achieving resolution when treated with corticosteroids and 80.6% with cryotherapy [20, 21]. The method frequently employed in clinical practice is cryotherapy utilizing liquid nitrogen, but this has inherent drawbacks such as tissue over-freezing resulting from an inability to achieve uniform energy distribution or scar formation [21, 25]. Furthermore, the therapeutic response is variable, often accompanied by disease relapse.

The purpose of this report is to understand the bioeffects of moderately dosed 20 MHz HIFU on the upper layer of human skin and compare it to results of cryotherapy commonly used in treatment of GA. These moderate levels of HIFU are below the threshold for direct ablation, but preclinical studies suggest that HIFU can induce immunogenic cell death and immune sensitization, potentially leading to generalized lesion regression and thereby a new modality for treatment of inflammatory skin conditions, including GA.

METHODS: NUMERICAL MODELLING

Finite Element Modelling

Analysis of the clinical response to HIFU at moderate energy exposures and conventional cryogenic spray treatment was performed using numerical modelling. FEM was used because of the complex nature of the interaction of the skin tissue with either focused acoustic waves or the heat flux due to the cryogenic spray. A three-layer model of human skin was used comprising of epidermis, dermis, and subcutaneous layer, having thickness of 0.1, 1.5 and 4.4 mm,

respectively [9]. The skin response was simulated using a sufficiently large axisymmetric computational domain representing a cylinder of 22 mm diameter, so that the calculated response was not affected by the employed boundary conditions. COMSOL Multiphysics version 5.4 FEM software (COMSOL AB, Stockholm Sweden) was used in all presented calculations.

Harmonic Pressure Field (HIFU)

The response of human skin to focused acoustic field was first calculated using harmonic pressure solver, and the pressure p, intensity I as well as heat source distribution Q_{ac} due to attenuation were calculated at nominal operating frequency $f_0 = 20.0$ MHz. The governing equation in this case is an inhomogeneous Helmholtz equation

where the losses in the media due to attenuation are introduced by the complex wave number and complex sound velocity. For clarity the details are omitted here; for more information one can refer to [26]. The attenuation in skin layers is frequency-dependent and is defined by the power law as follows [10]:

$$\alpha(f) = \alpha_0 \left(f/10^6\right)^{\eta}, \tag{1}$$

where α_0 is the attenuation coefficient, η is the power of the attenuation, frequency f is given in hertz. The dimensions of the simulated system as well as the boundary conditions are illustrated in Fig. 1A; material parameters are given in Table 1. The acoustic computational domain was meshed using an element size of maximum 1/10th of the wavelength in the proximity
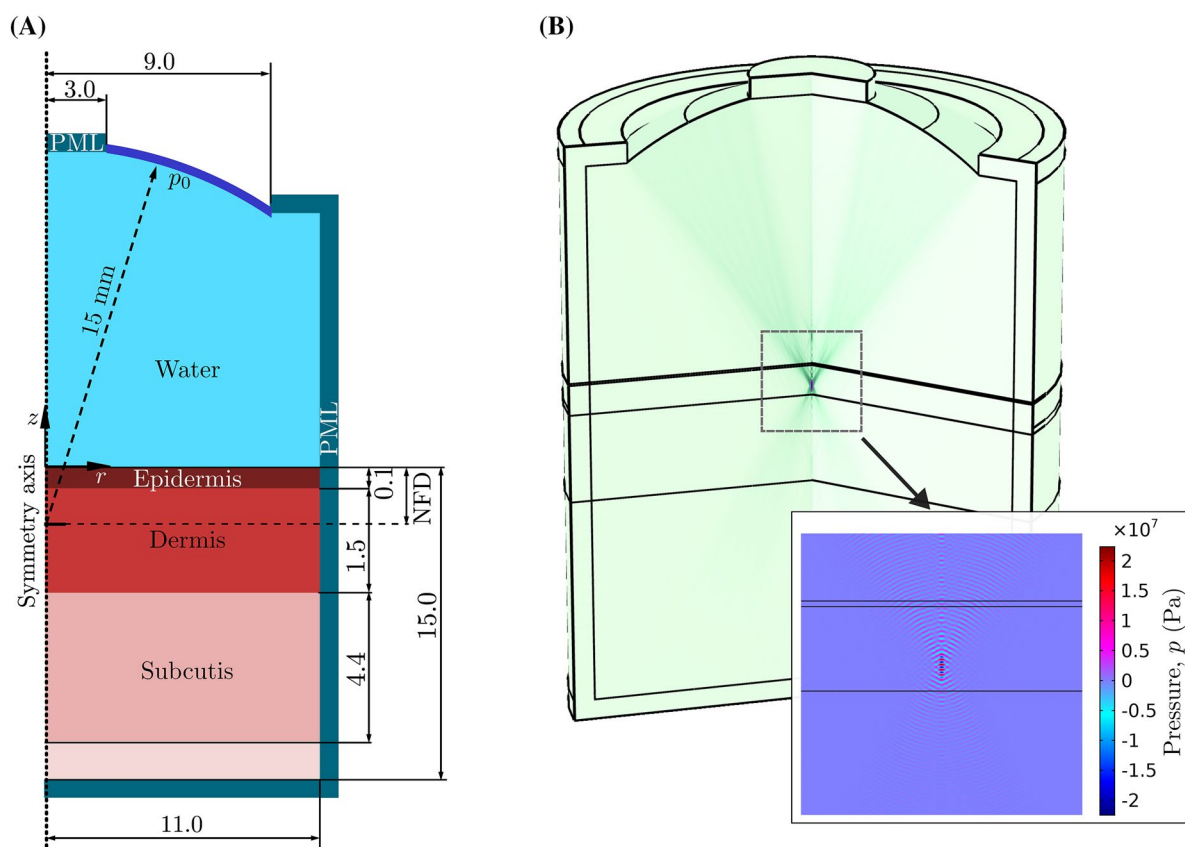

Fig. 1 A Dimensions and boundary conditions used in harmonic modelling of the ultrasonic field during high intensity focused ultrasound (HIFU) treatment of skin. Dimensions in mm. *NFD* nominal focal depth, *PML* perfectly matched layer. **B** Exemplary result of simulation of pressure field generated by a 20 MHz HIFU at $P_a = 3.33$ W, with NFD = 1.3 mm

Table 1 Model parameters of water and main skin components used in harmonic modelling of the acoustic field during high intensity focused ultrasound (HIFU) treatment

Parameter	Unit	Water	Epidermis	Dermis	Subcutis
Attenuation, α	dB/m/MHz	0.217	44.0 [41]	26.4 [41]	60.0 [42]
Attenuation exponent, η	–	2.00	1.55 [41]	1.69 [41]	1.00
Sound velocity, c	m/s	1482	1645 [41]	1595 [41]	1450 [42]
Density, ρ	kg/m^3	1000	1190 [9]	1116 [9]	971 [9]
Bulk modulus, K	GPa	2.20	3.22	2.84	2.04

diameter of 1.5 mm from the focal point, while the 1/5th of the wavelength rule was used outside of the focal zone in the remaining computational domain. The input acoustic power was introduced into the system through a pressure source boundary condition with the pressure value at the acoustic source surface p_0 (see Fig. 1) defined as:

$$p_0 = \sqrt{\frac{2\rho c P_a}{A}}, \qquad (2)$$

where ρ and c are the density and the sound velocity in water, P_a is the acoustic power defined by the exposure and A is the surface area of the radiating surface (the active surface of the piezoelectric transducer). Given the effective outer and inner diameters of the piezoelectric transducer are equal to 18 mm and 6 mm, respectively, the surface area $A = 254.2$ mm^2, in all simulated cases.

Transient Heat Transfer

The transient thermal response to HIFU and cryogenic spray exposure was calculated using the same general bio-heat transfer equation [27]:

$$\rho c_p(T)\frac{\partial T}{\partial t} = k(T)\nabla^2 T + Q_{met} + Q_{per}(T) + Q_{ext}(t), \qquad (3)$$

where T is the temperature, ρ is the density, c_p is the specific heat at constant pressure, Q_{met} is the metabolic heat generation and

$$Q_{per} = w_b c_{p,b}(T_b - T), \qquad (4)$$

is the heat transfer due to blood perfusion, where T_b is the temperature of blood, w_b is the perfusion rate and $c_{p,b}$ is the specific heat capacity of blood. The spatial dependence of T in Eqs. (3) and (4) is omitted for clarity. The thermal properties of the skin layers used in the simulations are given in Table 2.

The external heat transfer in case of the cryogenic spray freezing was represented by a heat flux boundary condition q_f as illustrated in Fig. 2A. The diameter of the heat flux on the skin was equal to 8.4 mm. This was estimated by considering typical application parameters i.e. the distance of 30 mm between the spray nozzle and the skin surface and assuming 16° far-field spray angle [28]. This value is consistent with the observations of the cold spot during clinical treatment using liquid nitrogen cryotherapy.

In the transient simulations the heat flux q_f was multiplied by a step function:

$$S(t) = \begin{cases} 1, & t \geq 0 \ and \ t < t_e \\ 0, & t \geq t_e \end{cases}, \qquad (5)$$

where t_e is the time of exposure.

In case of HIFU exposure, $Q_{ext} = Q_{ac}$, where Q_{ac} is the general heat source due to absorbed acoustic wave due to attenuation in the skin tissue given by:

$$Q_{ac} = 2\gamma\alpha(f)|I|, \qquad (6)$$

where $|I|$ is the magnitude of acoustic intensity as per the results of harmonic simulations of pressure field. In reality not all the attenuated ultrasound is converted into heat, which is included in Eq. (6) by introduction of the conversion coefficient $\gamma = 0.31$ [29]. Additionally, a

Table 2 Model parameters of water and main skin components used in transient modelling of the heat transfer during cryogenic spray and high intensity focused ultrasound (HIFU) treatments

Parameter	Unit	Water	Epidermis	Dermis	Subcutis
Heat capacity at constant pressure ($T \geq 0\ °C$), c_p	J/kg/K	4186*	3600 [9]	3300 [9]	2700 [9]
Heat capacity at constant pressure ($T < 0\ °C$), c_p	J/kg/K	2095 [43]	2501**	2420**	2258**
Thermal conductivity ($T \geq 0\ °C$), k	W/m/K	0.594*	0.235 [9]	0.445 [9]	0.185 [9]
Thermal conductivity ($T < 0\ °C$), k	W/m/K	2.2 [43]	1.669**	1.726**	1.656**

*Given values at 20 °C; however, the COMSOL default piecewise dependency on T was used in the actual simulations

**Estimated using values for $T \geq 0\ °C$, water properties at $T < 0\ °C$, assuming water content of 73% [44]
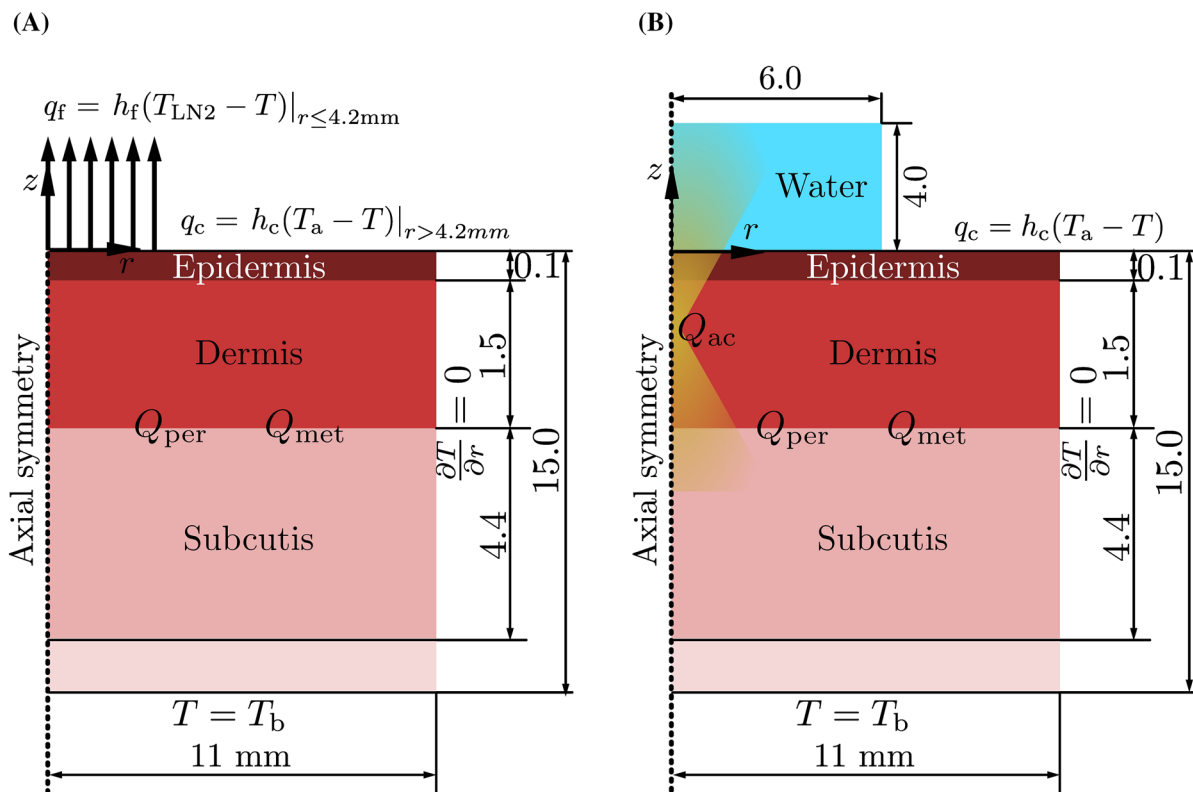

Fig. 2 Dimensions and boundary conditions used in the transient modelling of heat transfer. **A** Using cryogenic spray. **B** Using 20 MHz dermatological high intensity focused ultrasound (HIFU). Dimensions in mm; r and z, spatial coordinates; T, temperature; T_a, ambient temperature; T_b, blood temperature; T_{LN2}, temperature of liquid nitrogen; q_f, heat flux due to cryogenic freezing; q_c, convective heat flux; h_f, heat transfer coefficient of cryogenic freezing; h_c, convective heat transfer coefficient; Q_{per}, heat source due to blood perfusion; Q_{met}, metabolic heat source; Q_{ac}, heat source due to attenuation of the acoustic wave in tissue

volume of water was added to the computational domain above the HIFU exposure location (see Fig. 2B) to take into account the coupling water present in the HIFU handpiece during the HIFU exposure. Similarly to the cryotherapy, Q_{ac} was multiplied by a step function, Eq. (5).

Necrotic Dose Volume Estimation (HIFU)

In case of hyperthermia due to HIFU exposure, the definition of a dose is well defined and widely accepted [14, 30] and it is expressed in terms of thermally equivalent time by the following formula:

$$D_{\mathrm{H}}(\boldsymbol{x}, t) = \int_0^t R^{\left(T_{\mathrm{cr}} - T\left(\boldsymbol{x}, t'\right)\right)} \mathrm{d}t', \qquad (7)$$

where $R = 0.5$ for $T \geq 43$ °C. Moreover, $T_{\mathrm{cr}} = 43$ °C is the critical temperature for hyperthermia. It is accepted that once a tissue reaches the critical dose $D_{\mathrm{cr,H}} = 14,400$ s (equivalent of 240 min) 100% of cells undergo necrosis. The HIFU necrotic volume can therefore be expressed as:

$$V_{D,\mathrm{H}}(t) = \int_\Omega N(\boldsymbol{x}, t) \mathrm{d}V, \qquad (8)$$

where Ω is the computational domain, $x \in \Omega$ and selector function is defined according to the following formula:

$$N(\boldsymbol{x}, t) = \begin{cases} 1, & D_{\mathrm{H}}(\boldsymbol{x}, t) \geq D_{\mathrm{cr,H}} \\ 0, & D_{\mathrm{H}}(\boldsymbol{x}, t) < D_{\mathrm{cr,H}} \end{cases}. \qquad (9)$$

Another interesting indicator of the therapeutic process is the average temperature in the necrotic volume due to HIFU hyperthermia, also a function of time, defined in the following manner:

$$\overline{T}_{D,\mathrm{H}}(t) = \frac{\int_\Omega N(\boldsymbol{x}, t) T(\boldsymbol{x}, t) \mathrm{d}V}{V_{D,\mathrm{H}}(t)}. \qquad (10)$$

Necrotic Dose Volume Estimation (Cryotherapy)

There are no widely accepted standards regarding definition of necrotic volume due to the exposure to cryotherapy [31]; however, it is commonly accepted that once a living tissue reaches

the critical temperature of $T_{\mathrm{cr,C}} = -50$ °C it is certain that 100% of cells undergo necrosis. Therefore, in the present study the necrotic volume is defined by the volume of tissue surrounded by an isothermal surface, where $T(t) = T_{\mathrm{cr,C}}$. One needs to notice that such a volume is a function of time t and will decrease once the exposure stops. Of course, necrosis is a non-reversal process and therefore the cryogenic necrotic dose volume is calculated, as follows:

$$V_{D,\mathrm{C}}(t) = \max_{t' \in [0,t]} \int_\Omega M(\boldsymbol{x}, t') \mathrm{d}V, \qquad (11)$$

where Ω is the computational domain, $x \in \Omega$ and selector function is defined according to the following formula:

$$M(\boldsymbol{x}, t) = \begin{cases} 1, & T(\boldsymbol{x}, t) \leq T_{cr} \\ 0, & T(\boldsymbol{x}, t) > T_{cr} \end{cases}. \qquad (12)$$

Another interesting indicator of the therapeutic process is the average temperature in the necrotic volume, also a function of time, defined in the following manner:

$$\overline{T}_{D,\mathrm{C}}(t) = \frac{\int_\Omega M(\boldsymbol{x}, t) T(\boldsymbol{x}, t) \mathrm{d}V}{V_{D,\mathrm{C}}(t)}. \qquad (13)$$

RESULTS: NUMERICAL MODELLING

Transient Heat Transfer

A summary of the acoustic modelling of the HIFU field and estimation of the main characteristic is presented in Table 3. In all analysed exposure cases the spatial maximum intensity was located within the dermis layer as intended.

Here it should be mentioned that simulations of HIFU exposure are based on a linear acoustic model, which is only valid for limited levels of pressure $p \ll K$, where K is the bulk modulus. Given the values of bulk modulus K of the simulated tissue materials, summarized in Table 1, and the values of peak pressure presented in Table 3, one can, however, conclude that the use of the linear acoustic model is fully justified as the worst case is the exposure of NFD 0.8 mm and 0.6 J (4.00 W) resulting in peak pressure of

Table 3 Summary of the main characteristics of the acoustic field during high intensity focused ultrasound (HIFU) treatment for different exposure parameters

Exposure	Acoustic power	Maximum absolute pressure	Maximum magnitude of intensity	Location
	W	MPa	W/cm^2	
NFD0.8, 0.6 J	4.00	32.0	25,778	Dermis
NFD0.8, 0.4 J	2.67	26.1	17,137	Dermis
NFD1.3, 0.5 J	3.33	22.9	13,284	Dermis
NFD1.3, 0.3 J	2.00	17.7	7970	Dermis

Time of single exposure was equal to 0.15 s and it was the same for all HIFU treatments

NFD nominal focal depth

32.0 MPa which is almost a factor of 88 lower than the bulk modulus $K = 2.84$ GPa of dermis.

Thermal modelling of the skin response to exposure to the cryogenic spray and HIFU exposure was modelled for body and blood temperature $T_b = 37.0$ °C, and ambient temperature $T_a = 20$ °C. Perfusion rate $w_b = 0.00125$ kg/m^3/s for $T > 0$ °C [32], heat capacity of blood $c_{p,b} = 3770$ J/kg/m^3 [10]. Metabolic heat $Q_{met} = 368.1$ W/m^3 was set only in the dermis and subcutaneous layers [12]. The convective heat transfer coefficient h_c was equal to 3.3 W/m^2/K [33].

The heat flux due to the cryogenic spray was modelled by a heat flux where the cryogenic heat transfer coefficient $h_f = 4000$ W/m^2/K [34] and the temperature of the liquid nitrogen spray $T_{LN2} = -196$ °C (see Fig. 2A). Results of the transient development of necrotic dose volume and average temperature within necrotic dose volume, defined by Eqs. (11) and (13), respectively, are given in Fig. 3. To present the results for all the simulated treatment modalities the transient results are given using normalized time τ, defined as follows:
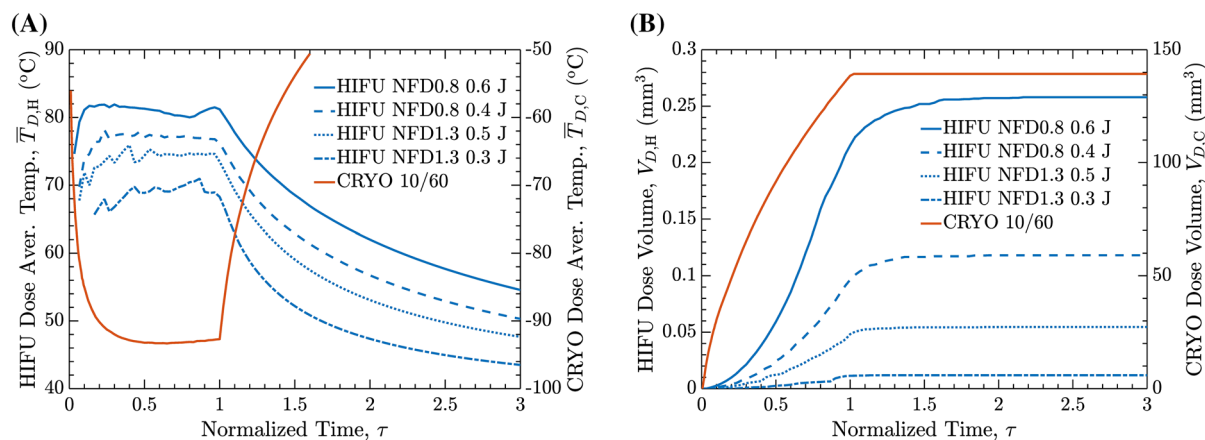
$$\tau = \frac{t}{t_e}. \tag{14}$$

Fig. 3 Results of the modelling of transient heat transfer during cryogenic spray treatment and high intensity focused ultrasound (HIFU) treatment of skin. **A** Spatial average temperature of the dose as a function of normalized time at different treatment parameters. **B** Necrotic dose volume as a function of normalized time at different treatment parameters. *NFD* nominal focal depth, *CRYO* cryotherapy

Heat Distribution and Necrotic Dose Volume

Temperature distribution at $t=10$ s ($\tau=1$) for skin exposure to liquid nitrogen spray is presented in Fig. 4A, while the cryogenic necrotic volume is visualized in Fig. 4F. Figure 3 shows the transient development of the necrotic volume as well as the average temperature of the necrotic volume induced by the HIFU exposure given by Eqs. (7) and (8), respectively. The HIFU exposure is determined by a number of parameters, namely nominal focal depth (NFD), which determines the location of the acoustic focus below the surface of the skin, acoustic power P_a which in combination with the exposure time t_e determines the total energy of a single exposure $E_e=P_a \cdot t_e$.

The following HIFU exposure parameters were used in the calculations: NFD0.8 $E_e=0.6$ J, NFD0.8 $E_e=0.4$ J, NFD1.3 $E_e=0.5$ J, NFD1.3 $E_e=0.3$ J. Here, NFD0.8 is understood as HIFU exposure at nominal focal depth of 0.8 mm, similarly NFD1.3 is a HIFU exposure at nominal focal depth of 1.3 mm. Additionally, the temperature distributions at $t=0.15$ s ($\tau=1$) due to the modelled single HIFU exposures are given in Fig. 4B–E. The necrotic volume at $t=0.5$ s (total time of simulation) as the results of HIFU exposure is visualized in Fig. 4G–J.

CASE ILLUSTRATION: GRANULOMA ANNULARE

A 47-year-old woman presented to the clinic with multiple lesions of GA on hands and forearms. The subject had undergone several cryotherapy treatments, and most recently received corticosteroid therapy 6 months prior to the HIFU treatment; however, the treatment outcomes were unsatisfactory, and the disease recurred. The subject therefore requested alternative treatments. Test treatments using cryotherapy was offered as the device-based standard of care in direct comparison with HIFU treatment as a potentially more effective and less painful therapeutic option. On the basis of agreement with the patient, 22 smaller lesions/sections on the posterior side of the hands and right forearm were selected as test areas for HIFU and 10 areas for comparative standard cryotherapy.

The Declaration of Helsinki's guiding principles were followed in the creation of this article. An ethical approval from Bioethical Review Board at Wroclaw Medical University, Poland (no. KB109/2023) has been obtained in compliance with local law and institutional norms to undertake this study. The authors attest that the patient's written consent has been received for the submission and publishing of this report, including the data and photographs.

Dermoscopy

The clinical evaluation of GA lesions was conducted through dermoscopy using a FotoFinder Medicam 1000 device (FotoFinder Systems GmbH, Bad Birnbach, Germany). The observed lesions of GA displayed typical characteristics before treatment: annular or arciform configuration with central clearing, a slightly raised border (Figs. 5A, B and 6A, B). Additionally, some lesions showed whitish or yellowish areas, fine peripheral scales, and telangiectasias.

HIFU Treatment

HIFU treatments were performed using a System ONE-M (TOOsonix A/S, Hoersholm, Denmark) operating at 20 MHz, designed specifically for dermatological applications. Four handpieces with nominal focal depth (NFD) of 0.8–2.3 mm below the skin surface are available for connection to the device. The handpieces include an integrated high-resolution digital camera operating as a dermoscope to observe the treated area in real time on the user screen. The high spatial resolution of the ultrasound field combined with the real-time dermoscopy ensures precise dosing of the therapeutic energy into the selected location on the GA lesions.

In situations where the targeted lesion is anticipated to be challenging to visualize because of insufficient contrast with the adjacent skin, the lesion can be marked using a water-resistant pen.

HIFU treatments of the 22 smaller GA fields were carried out by administering acoustic
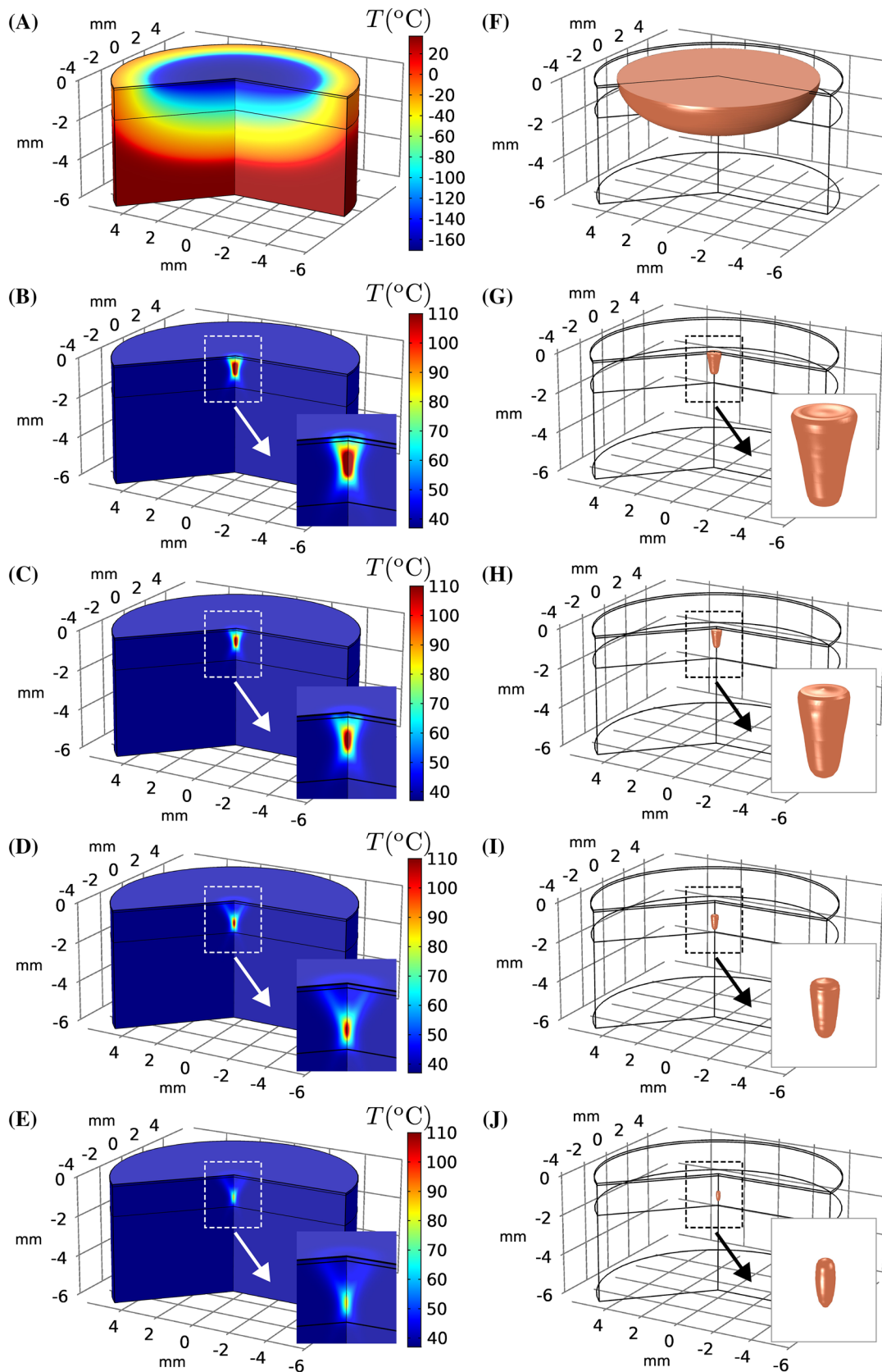
◄**Fig. 4** Results of transient heat transfer modelling of skin treatment using cryotherapy and high intensity focused ultrasound (HIFU). **A** Temperature field in around cryogenic spray exposure 10 s freeze 60 s thaw at $t = 10.0$ s. **B** Temperature field around NFD0.8/0.6 J HIFU exposure at $t = 0.15$ s. **C** Temperature field around NFD0.8/0.4 J HIFU exposure at $t = 0.15$ s. **D** Temperature field around NFD1.3/0.5 J HIFU exposure at $t = 0.15$ s. **E** Temperature field around NFD1.3/0.3 J HIFU exposure at $t = 0.15$ s. **F** Dose volume in response to cryogenic spray exposure 10 s freeze 60 s thaw at $t = 10.0$ s. **G** Dose volume in response to NFD0.8/0.6 J HIFU exposure at $t = 0.5$ s. **H** Dose volume in response to NFD0.8/0.4 J HIFU exposure at $t = 0.5$ s. **I** Dose volume in response to NFD1.3/0.5 J HIFU exposure at $t = 0.5$ s. **J** Dose volume in response to NFD1.3/0.3 J HIFU exposure at $t = 0.5$ s. *NFD* nominal focal depth

energy in bursts of 0.3–0.6 J/exposure at exposure durations of 0.15 s with approximately 0.75–1.5 mm spacing between each exposure site to cover the selected lesion field and a peripheral margin of approximately 1 mm. Visual appearance of the different spacings between each exposure site is illustrated in Fig. 7.

Two different HIFU handpieces of nominal focal depth 0.8 mm and 1.3 mm were used, thus limiting the treatment to the epidermis and upper third of the dermis. Standard ultrasound gel was used to provide acoustic coupling between the handpiece and skin surface (Parker Aquasonic 100, Parker Laboratories Inc, NJ, USA). The progress and status of the treatment were monitored in real time using the integrated non-polarized dermoscopic imaging system. On the basis of prior experience, no pre-treatment topical or local intravascular anaesthesia was used. HIFU treatments were conducted in two separate sessions with regular follow-up visits over the following 3 months.

HIFU-treated GA lesions showed an immediate circular whitening effect of approximately 2 mm around each targeted location (Fig. 5C, D). This effect was attributed to the denaturation of proteins in the affected cells and a partial release of the epidermal layer due to the rapid local temperature increase. After treating larger areas, a mild erythema appeared in the treatment field area as the result of an urticarial histamine release. This reaction gradually decreased over the following 1–2 h and did not

cause notable pain or discomfort for the subject. Approximately 6 days after HIFU treatment a crustation appeared, revealing centrally ulcerated areas with evident signs of smaller internal bruising (Fig. 5E, F). The vessels exhibited a dot-like linear arrangement radiating from the central part. The sites exposed directly to the HIFU shots presented amorphous white areas/spots. Shallow crusts with traces of blood were observed in the central region. During the healing process, the vascularity and fibrotic changes gradually became less pronounced (Fig. 5G, H), eventually leading to nearly healthy skin (Fig. 5I, J).

Cryotherapy

Liquid nitrogen cryotherapy was carried out on eight smaller GA fields located on the mid-section of the left posterior hand. A CRY-AC apparatus (Brymill Cryogenic Systems Inc, CT, USA) mounted with a 2-mm nozzle was used for application of liquid nitrogen spray onto the affected skin areas. The treatment temperature was maintained at approximately – 196 °C. Within the scope of the study, a single freeze–thaw cycle was administered, allowing the tissue to naturally undergo full thawing. The duration of cryotherapy was tailored to individual patient characteristics. Typically, the procedure lasted 10 s with 60 s thaw and involved a singular spray application with nozzle-to-skin distance of 30 mm.

The freeze–thaw cycle of cryotherapy was poorly evaluated by the patient, reporting intense pain. Following the procedure, urticarial post-frost blisters were observed (Fig. 6C, D). After a week, scabs and blisters filled with serous fluid appeared (Fig. 6E, F), with some of them ruptured. During the subsequent visit, the lesions were healed, but a side effect in the form of a significant scar emerged (Fig. 6G, H). In the surrounding area of the cryotherapy-treated site, a reticulate hyperpigmentation occurred, associated with the reparative response.

The HIFU and cryotherapy sessions as well as their parameters are summarized in Table 4.

(A)

(B)

(C)

(D)

(E)

(F)

(G)

(H)

(I)

(J)
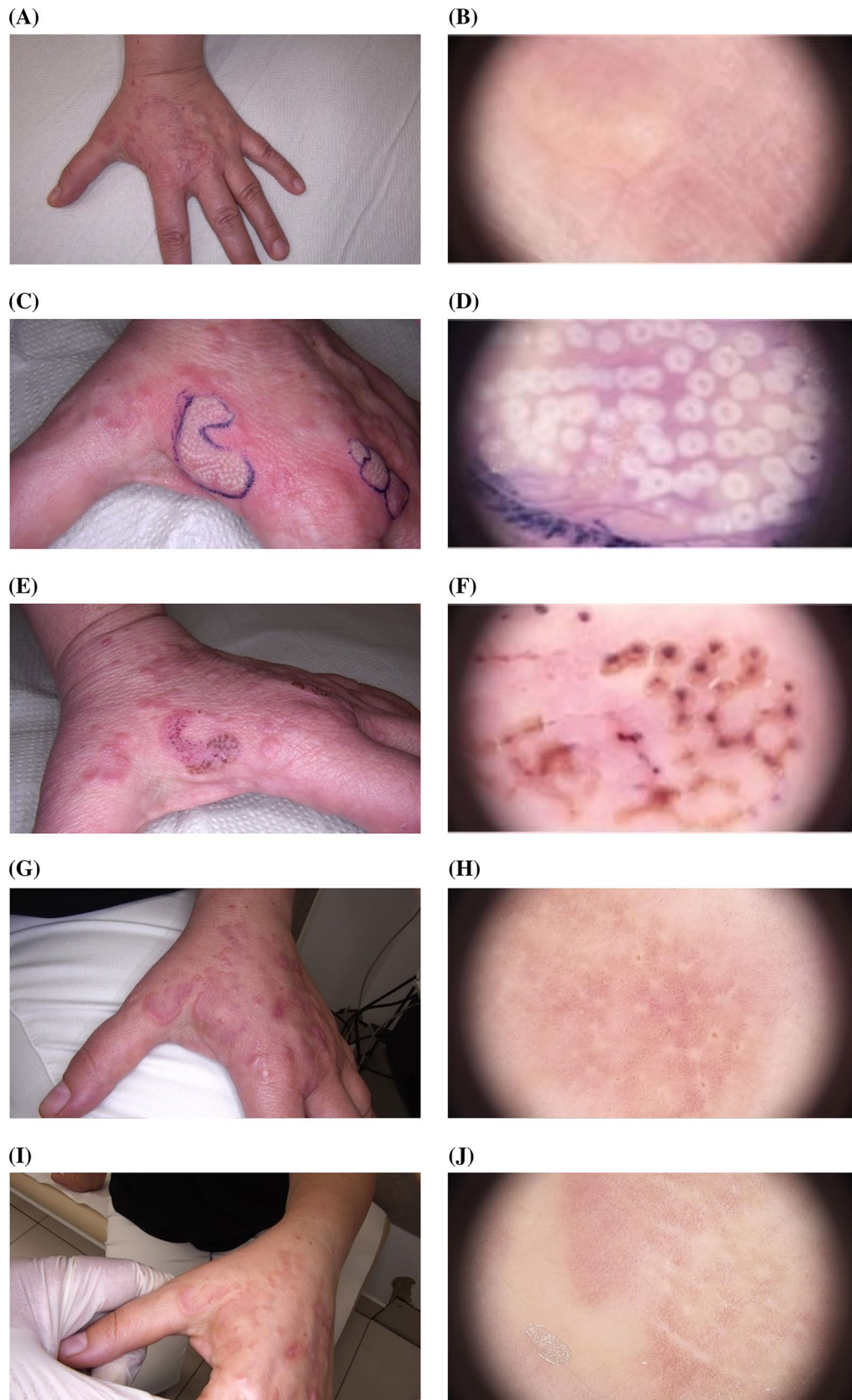
◄**Fig. 5** High intensity focused ultrasound (HIFU) treated lesions on left hand, NFD0.8 0.6 J 1.0 mm spacing. **A** Macroscopic view. **B** Dermoscopy before treatment. **C** Macroscopic view just after treatment. **D** Dermoscopy just after treatment. **E** Macroscopic view 6 days after treatment. **F** Dermoscopy 6 days after treatment. **G** Macroscopic view 27 days after treatment. **H** Dermoscopy 27 days after treatment. **I** Macroscopic view 93 days after treatment. **J** Dermoscopy 93 days after treatment. *NFD* nominal focal depth

DISCUSSION

The employed modelling methodology introduced in this report is a simplified representation of the biophysical process taking place during HIFU treatment and cryotherapy respectively, especially after the physiological response of the skin commences. Model output can, however, clearly illustrate the fundamental and significant resulting differences between the two methods, and the model can therefore be a very helpful tool for analysing observations from clinical treatments, such as the presented case of treatment of GA.

Figure 3 and Table 5 show results of the modelled average temperature and volume of the necrotic zone as a function of normalized time, up to three times the exposure time of the respective therapies applied in the GA case (3 × 150 ms for HIFU and 3 × 10 s for cryotherapy). As expected, the average temperature for cryotherapy rapidly decreases to reach a peak minimum of – 92.7 °C, and abruptly increases towards normal skin temperature as spray exposure is stopped. It has to be emphasised that the cooling rate is predetermined by the heat transfer coefficient h_f, which has been reported to vary up to three orders of magnitude between 10^3 and 10^6 W/m^2/K [35]. The value of $h_f = 4000$ W/m^2/K is therefore on the low side of this range and suggests that the reported estimates of the necrotic volume due exposure to nitrogen spray are conservative. Moreover, the obtained cooling rates are consistent with the experimental data obtained on gel phantoms [32, 36]. For HIFU, the average temperature of the necrotic volume quickly increases to stable levels of 68.3 to 81.2 °C depending on selected power setting of the exposure, and subsequently gradually decreases towards normal skin temperature after the exposure is stopped.

Bioeffects measured in necrotic volume due to single exposure to HIFU and liquid nitrogen spray are significantly different for both modalities. This effect is reflected clearly in the size of the necrotic volume shown in Fig. 3B. Here it can be observed that the necrotic zone following cryotherapy is several factors greater than those observed for a HIFU dose, exemplified by 138.5 mm^3 for cryotherapy and a maximum 0.258 mm^3 for a single HIFU dose. This difference is of course offset by multiplications of HIFU exposures needed to cover an equivalent treatment area, but it underlines the highly improved accuracy and resolution in both lateral and horizontal directions offered by the HIFU modality.

The temperature distribution in the tissue and the necrotic volumes are presented in more detail in Fig. 4. Again, the zone of hypothermic impact can initially be seen to be very large in the case of single cryotherapy spray exposure (Fig. 4A) compared to the single exposures from the various HIFU settings (Fig. 4B–E). This is directly reflected in the visualization of the necrotic volume (Fig. 4F–J), thereby also illustrating the single exposure modality for cryotherapy versus the need for multiple exposures to conduct a full treatment with HIFU. Moreover, it can be concluded that even at the densest spacing of HIFU exposures (0.75 mm) the total impact of a multidose exposure can be analysed as a superposition of single exposures, due to very confined temperature distribution of a single HIFU exposure.

Table 6 summarizes and analyses clinical records from the GA treatments combined with the modelled necrotic volumes shown in Figs. 3, 4 and Table 5. It can first of all be noticed that the total necrotic volume created by the relevant repetitions of HIFU exposures is only 0.53–11.5% of a necrotic volume created by a single cryotherapy spray exposure. The necessity for repetitive HIFU exposures to cover the relevant target, however, potentially also increases treatment time. The maximum effective treatment time was thus approximately three times (297%) longer than the single
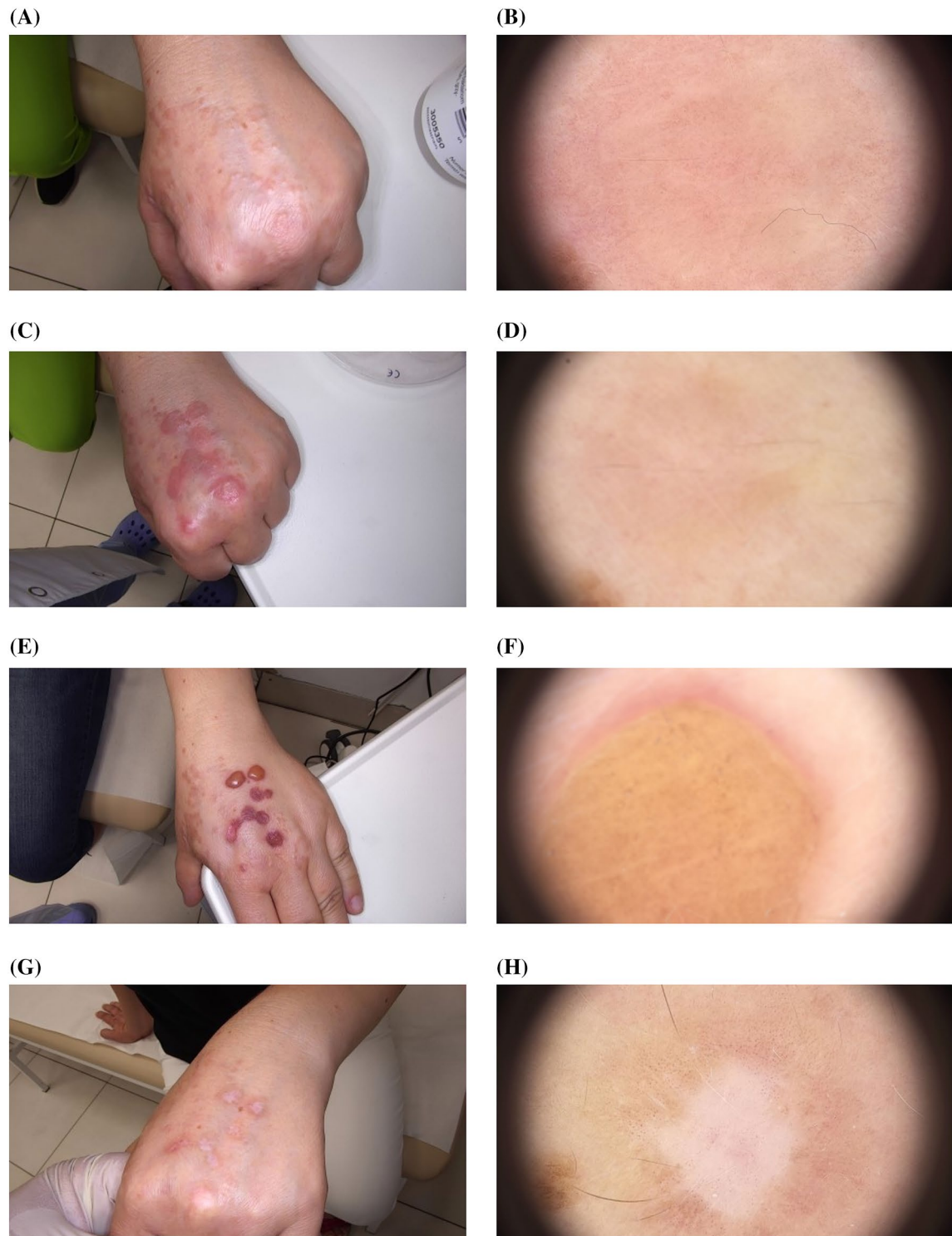
Fig. 6 Cryotherapy treated lesion on left hand. **A** Macroscopic view before treatment. **B** Dermoscopy before treatment. **C** Macroscopic view just after treatment. **D** Dermoscopy just after treatment. **E** Macroscopic view 5 days after treatment. **F** Dermoscopy 5 days after treatment. **G** Macroscopic view 34 days after treatment. **H** Dermoscopy 34 days after treatment
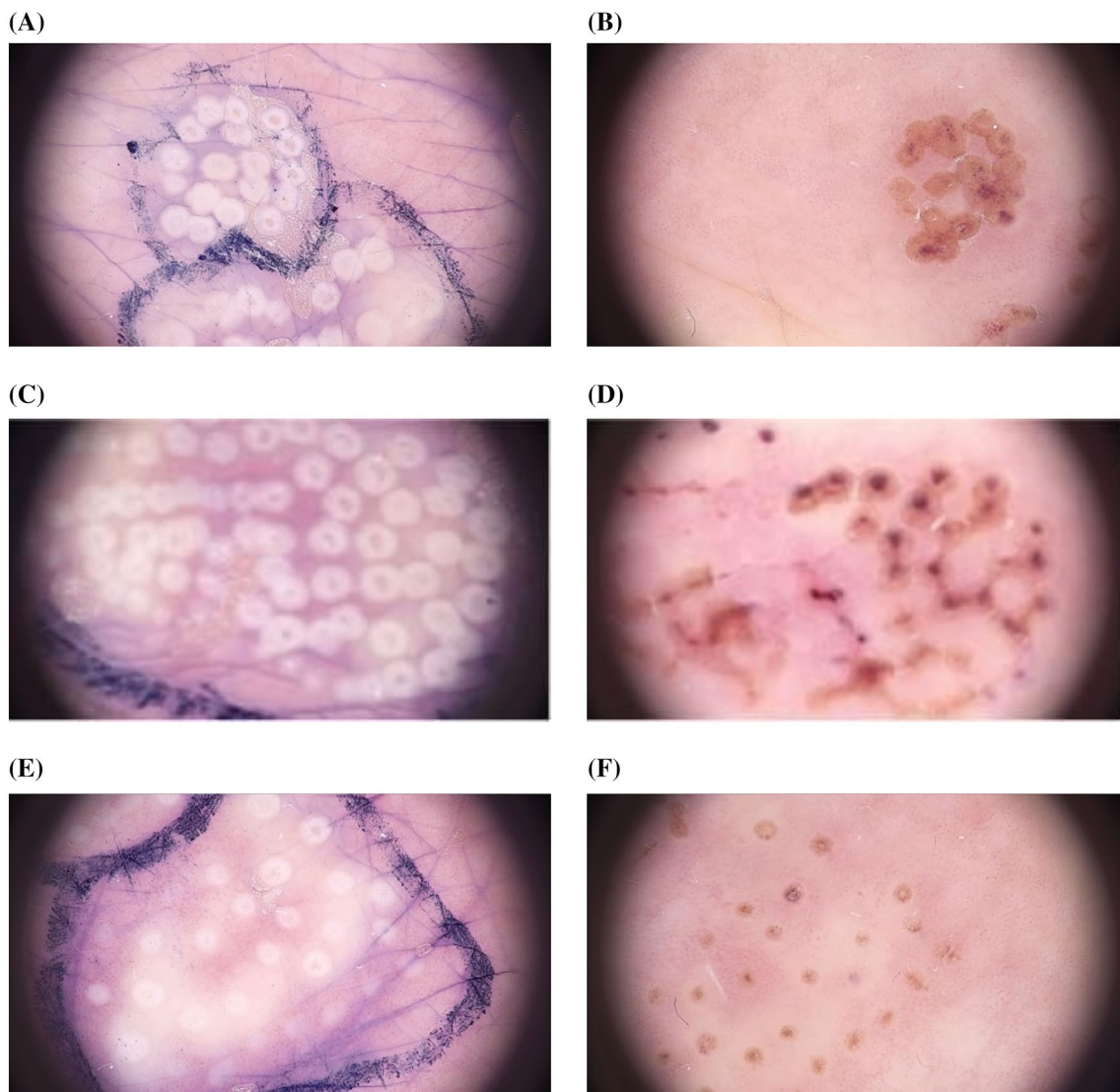
Fig. 7 Dermoscopic image of granuloma annulare (GA) treated with high intensity focused ultrasound (HIFU) at nominal focal depth (NFD) NFD0.8 0.4 J with 0.75 mm average spacing of exposures **A** just after treatment and **B** 6 days after treatment. Dermoscopic image of GA treated with HIFU at NFD0.8 0.6 J with 1.0 mm average spacing of exposures **C** just after treatment and **D** 6 days after treatment. Dermoscopic image of GA treated with HIFU at NFD0.8 0.4 J with 1.5 mm average spacing of exposures **E** just after treatment and **F** 6 days after treatment

cryotherapy cycle time—a time consumption that is, however, well within acceptable limits and not expected to effectively impact the total time needed for a clinical session including record review, diagnosis, registration, clinical setup, post-treatment registration, etc.

Examples of clinical results and observations, shown in Figs. 5 and 6 with a summary in Table 4, indicate relatively scattered clinical results as would be expected for a first treatment in a single patient only. However, as previously reported [1] and predicted by the numerical models, cryotherapy creates large necrotic volumes in the skin. Observed diameters of necrotic volumes showing diameters around 8.4 mm on the skin surface match modelled results very

Table 4 Summary of the treatment sessions, parameters of treatment and results

Session	Location	Exposure	Exposure average spacing (mm)	Follow-up (days)	Number of lesions	Results	Biological response
1	Left hand	HIFU NFD0.8 0.4 J	1.0	93	1	Full recovery	Minimal crust formation and the slightest pigmentation alteration
1	Left hand	HIFU NFD0.8 0.4 J	1.5	93	1	Full recovery	Moderate crust formation and moderate pigmentation alteration
1	Left hand	HIFU NFD0.8 0.4 J	0.75	93	1	Full recovery	Significant crust formation and extensive pigmentation alteration
1	Left hand	HIFU NFD0.8 0.6 J	1.0	93	2	Full recovery	Significant crust formation and the most extensive pigmentation alteration
1	Left hand	HIFU NFD0.8 0.6 J	1.0	93	1	Partial recovery	Significant crust formation and the most extensive pigmentation alteration
1	Right hand	HIFU NFD1.3 0.3 J	0.75	93	1	Partial recovery	Minimal crust formation
1	Right hand	HIFU NFD1.3 0.3 J	1.0	93	1	Partial recovery	Moderate crust formation
1	Right hand	HIFU NFD1.3 0.5 J	1.5	93	3	Full recovery	Significant crust formation in the form of semicircles
2	Right forearm	HIFU NFD1.3 0.5 J	1.0	73	10	Full recovery	Moderate pigmentation alteration

Table 4 continued

Session	Location	Exposure	Exposure average spacing (mm)	Follow-up (days)	Number of lesions	Results	Biological response
2	Right forearm	HIFU NFD1.3 0.5 J	1.0	73	1	Partial recovery	Significant crust formation and extensive pigmentation alteration
3	Left hand	CRYO 10/60	N/A	34	8	Full recovery	Frostbite blisters that ruptured, resulting in a large crust build-up. Substantial scar formation with hypopigmentation at the periphery

HIFU high intensity focused ultrasound, *NFD* nominal focal depth, *CRYO* cryotherapy, *N/A* not applicable

Table 5 Summary of the numerical dose estimations in response to all combinations of exposure parameters used in the clinic for cryogenic spray and high intensity focused ultrasound (HIFU) treatments

Exposure parameters	Exposure time, s	Single dose necrotic volume, mm^3 (μl)	Dose average temperature at $\tau = 1$, °C
CRYO 10/60	10.0	138.5	− 92.7
HIFU NFD0.8, 0.6 J	0.15	0.258	81.2
HIFU NFD0.8, 0.4 J	0.15	0.118	76.2
HIFU NFD1.3, 0.5 J	0.15	0.055	73.5
HIFU NFD1.3, 0.3 J	0.15	0.012	68.3

CRYO cryotherapy, *NFD* nominal focal depth

well (Fig. 4A). Similarly, the simulated necrotic zone created by HIFU having an outer ring and centre spot on the skin surface when using an NFD 0.8 mm handpiece is fully reflected in clinical observations (Fig. 4D).

Importantly, all HIFU treatments using a handpiece with NFD 0.8 or 1.3 mm is generally found to lead to full or partial resolution in all treated fields. The initial indication is thus that the suggested immunological activation induced by hyperthermic HIFU indeed leads to generalized lesion regression without full ablation of

the lesion field as suggested in the preclinical studies [5–7]. The method therefore seems to be a viable pathway for future treatment of inflammatory conditions in humans.

The HIFU method is furthermore found to present a significantly improved clinical balance over cryotherapy, with less scarring and dyspigmentation. Treatments using energy levels of 0.3 J/exposure seem to be close to the lower threshold for observable clinical effect, while 0.6 J/exposure creates larger coherent crustations and subsequent dyspigmentation unless

Table 6 Summary of the analysis of the equivalent total high intensity focused ultrasound (HIFU) dose volumes to a single cryogenic spray treatment exposing 8.4 mm dimeter area of skin to liquid nitrogen for 10 s

Exposure	Exposure average spacing	Equivalent number of HIFU exposures to single CRYO	Total equivalent dose volume	Ratio of total volume of HIFU dose to CRYO dose	Total treatment time	Ratio of total HIFU treatment time to single CRYO exposure
	mm	–	mm^3 (µl)	%	s	%
CRYO 10/60	N/A	N/A	138.5	100	70	100
HIFU NFD0.8, 0.4 J	1.00	62	7.33	5.29	124	177
HIFU NFD0.8, 0.4 J	1.50	31	3.66	2.65	62	89
HIFU NFD0.8, 0.4 J	0.75	104	12.29	8.87	208	297
HIFU NFD0.8, 0.6 J	1.00	62	15.99	11.5	124	177
HIFU NFD1.3, 0.3 J	0.75	104	1.23	0.89	208	297
HIFU NFD1.3, 0.3 J	1.00	62	0.74	0.53	124	177
HIFU NFD1.3, 0.5 J	1.50	31	1.69	1.22	62	89
HIFU NFD1.3, 0.5 J	1.00	62	3.39	2.45	124	177

CRYO cryotherapy, *NFD* nominal focal depth, *N/A* not applicable

used with larger spacing between each exposure. Energy levels of 0.4–0.5 J/exposure and a spacing of 1.0 mm, however, seem to have a good clinical balance with full recovery of the skin and relatively low levels of dyspigmentation seen in 15 out of 17 treated lesions using this energy range. Somewhat outside documented clinical data, the recommendation is furthermore that applying a 1-mm margin yielded better results for reduction of GA, as the absence of this margin resulted in some lesions persisting as raised areas.

Overall, these observations match earlier reported preclinical results [3, 37, 38], as well as observations in clinical work, where only energy levels above 0.7 J/exposure were found to initiate the desired direct ablative effects [2, 3, 39].

As a result of the limited follow-up (less than 12 months) it is difficult to speculate about the possibility of relapse of GA in the long-term perspective after both HIFU and cryotherapy treatment. As of the date of the latest version of this report (approximately 9 months after treatment) no recurrences were observed in the pathologically altered areas treated with HIFU. However, this was not the case in the GA lesions subjected to cryotherapy. Although it is an interesting finding, a more systematic study needs to the carried out to further confirm this phenomenon.

Areas of frequent occurrence of GA, such as the skin on hands, feet, knees, or back, can confidently undergo HIFU therapy. Facial locations have not been studied. However, given the very positive cosmetic outcome of HIFU treatment of

the areas presented in this report one might suspect that HIFU can also be successfully applied to such areas. Furthermore, as a result of the physical dimensions of the handpiece, HIFU cannot be applied to lesions located on the oral mucosa. Similarly, no studies have been conducted in the anogenital region.

The main limitation of the study is the limited data obtained by only having a single patient in this first evaluation and comparison between the two therapeutic methods. Further studies with larger populations are needed for full statistical analysis, in particular when analysing the HIFU treatment modality where no prior data or experience exist for GA or other inflammatory skin diseases. As mentioned above, the data is further limited by conducting treatments on the hands and forearms only, whereas skin response and healing dynamics are generally known to be dependent on anatomical location. Similarly, the exposure parameters selected for both cryotherapy and HIFU treatments were of limited range. In particular, a limitation in the presented data was not examining a larger range of HIFU energy settings, which might have provided a more nuanced view of application and potential contraindications for treatments on different patients and anatomical locations. The use of a linear model in modelling of the thermal response of skin to HIFU field, where non-linear effects such as temperature dependence of skin parameters or phase change have not been considered, is another limitation of the presented study.

CONCLUSIONS

This report is aimed at understanding the bioeffects created by moderately dosed 20 MHz HIFU, i.e. energy levels of 0.3–0.6 J/exposure to the upper layer of the human skin. This is compared with effects generated by cryotherapy, a device-based therapy commonly used in dermatology, including in the treatment of inflammatory skin conditions.

These moderate levels in HIFU are below the threshold for creating larger coherent necrotic effects used for direct treatment of e.g. BCC or actinic keratosis, but preclinical studies using HIFU suggest that local ablative techniques can induce immunogenic cell death (ICD), increased tumour infiltration by macrophages, as well as CD4^{+} and CD8^{+} lymphocytes [5]. Therefore, HIFU can also effectively induce immune sensitization, which contributes to more generalized lesion regression [5, 6, 37].

Numerical modelling was used to analyse the clinical response from HIFU and conventional cryogenic spray treatment. This was obtained by a FEM including the interaction of the skin tissue with either focused acoustic waves or the heat flux due to the cryogenic spray. A three-layer model of human skin was used comprising epidermis, dermis, and subcutaneous layer, having thickness of 0.1, 1.5 and 4.4 mm, respectively.

The model output showed that 20 MHz HIFU can be accurately adjusted to affect very small and accurately positioned lesions in the upper dermis, thus creating local necrotic volumes that are several times smaller than those created by cryotherapy.

The model output results were compared to clinical results observed from treatment of a patient with the inflammatory disease GA actively seeking improved therapeutic options after unsatisfactory results with corticosteroids. While the data from this single patient is extremely limited, important confirmation of the proposed new methodology was obtained. All 22 lesions treated by HIFU indicated full or partial recovery of the skin, and significantly less scarring and dyspigmentation than in the lesions treated by cryotherapy.

In conclusion, the treatment of inflammatory conditions in humans using HIFU exposures slightly below the threshold leading to a combined ablative treatment response presents significant advantages over the otherwise commonly used cryotherapy, including reduced scarring and dyspigmentation. Optimal HIFU energy levels of 0.4–0.5 J/exposure with a spacing of 1.0 mm demonstrate a favourable clinical balance, resulting in full skin recovery and minimal dyspigmentation. Further work on additional patients with GA as well as other inflammatory skin conditions is strongly encouraged to investigate these positive results

further. There is a substantial body of research demonstrating that HIFU enhances the membrane permeability and therefore it can be of a significant assistance also during drug delivery [40]. Combination treatment using HIFU with pharmaceutical treatment is therefore an obvious and interesting option for further investigation.

ACKNOWLEDGEMENTS

We thank the patient for participating in this study.

Declarations

REFERENCES

1. James WD, Berger TG, Elston DM, et al. Andrews' diseases of the skin: clinical dermatology. Twelfth edition. Philadelphia, PA: Elsevier; 2016. https://www.clinicalkey.com/dura/browse/bookChapter/3-s2.0-C20120068895. Accessed 3 Apr 2024.

2. Calik J, Migdal M, Zawada T, et al. Treatment of seborrheic keratosis by high frequency focused ultrasound—an early experience with 11 consecutive cases. Clin Cosmet Investig Dermatol. 2022;15:145–56.

3. Serup J, Bove T, Zawada T, et al. High-frequency (20 MHz) high-intensity focused ultrasound: new treatment of actinic keratosis, basal cell carcinoma, and Kaposi sarcoma. An open-label exploratory study. Skin Res Technol. 2020;26:824–31.

4. Seyed Jafari SM, Cazzaniga S, Bossart S, et al. Efficacy assessment of the high-frequency high-intensity focused ultrasound as a new treatment for actinic keratosis. Dermatology. 2022;238:662–7.

5. Fite BZ, Wang J, Kare AJ, et al. Immune modulation resulting from MR-guided high intensity focused ultrasound in a model of murine breast cancer. Sci Rep. 2021;11:927.

6. van den Bijgaart RJE, Mekers VE, Schuurmans F, et al. Mechanical high-intensity focused ultrasound creates unique tumor debris enhancing dendritic cell-induced T cell activation. Front Immunol. 2022. https://doi.org/10.3389/fimmu.2022.1038347.

7. Eranki A, Srinivasan P, Ries M, et al. High-intensity focused ultrasound (HIFU) triggers immune sensitization of refractory murine neuroblastoma to checkpoint inhibitor therapy. Clin Cancer Res. 2020;26:1152–61.

8. Silva M, Freitas B, Andrade R, et al. Computational modelling of the bioheat transfer process in human skin subjected to direct heating and/or cooling sources: a systematic review. Ann Biomed Eng. 2020;48:1616–39.

9. Xu F, Lu TJ, Seffen KA, et al. Mathematical modeling of skin bioheat transfer. Appl Mech Rev. 2009;62. https://cir.nii.ac.jp/crid/1361418518794014976.

10. Gupta P, Srivastava A. Numerical analysis of thermal response of tissues subjected to high intensity focused ultrasound. Int J Hyperthermia. 2018;35:419–34.

11. Marin M, Hobiny A, Abbas I. Finite element analysis of nonlinear bioheat model in skin tissue due to external thermal sources. Mathematics. 2021;9:1459.

12. Bhowmik A, Repaka R, Mishra SC. Thermal analysis of the increasing subcutaneous fat thickness within the human skin—a numerical study. Num Heat Transfer Part A. 2015;67:313–29.

13. Damianou CA, Hynynen K, Fan X. Evaluation of accuracy of a theoretical model for predicting the necrosed tissue volume during focused ultrasound surgery. IEEE Trans Ultrason Ferroelectr Freq Control. 1995;42:182–7.

14. Shaw A, ter Haar G, Haller J, et al. Towards a dosimetric framework for therapeutic ultrasound. Int J Hyperth. 2015;31:182–92.

15. Schmieder SJ, Harper CD, Schmieder GJ. Granuloma annulare. StatPearls. Treasure Island (FL): StatPearls; 2023. http://www.ncbi.nlm.nih.gov/books/NBK459377/.

16. Joshi TP, Duvic M. Granuloma annulare: an updated review of epidemiology, pathogenesis, and treatment options. Am J Clin Dermatol. 2022;23:37–50.

17. Barbieri JS, Rodriguez O, Rosenbach M, et al. Incidence and prevalence of granuloma annulare in the United States. JAMA Dermatol. 2021;157:1–8.

18. Stewart LR, George S, Hamacher KL, et al. Granuloma annulare of the palms. Dermatol Online J. 2011;17. https://escholarship.org/uc/item/5kg28155.

19. Mempel M, Musette P, Flageul B, et al. T-cell receptor repertoire and cytokine pattern in granuloma annulare: defining a particular type of cutaneous granulomatous inflammation. J Investig Dermatol. 2002;118:957–66.

20. Cichoń M, Placek WJ. Granuloma annulare—diagnostic challenges. Dermatology Review/Przegląd Dermatologiczny. 2022;109:368–90.

21. Wang J, Khachemoune A. Granuloma annulare: a focused review of therapeutic options. Am J Clin Dermatol. 2018;19:333–44.

22. Rubin CB, Rosenbach M. Granuloma annulare: a retrospective series of 133 patients. Cutis. 2019;103:102–6.

23. Nordmann TM, Kim J-R, Dummer R, et al. A monocentric, retrospective analysis of 61 patients with generalized granuloma annulare. Dermatology. 2020;236:369–74.

24. Khanna U, North JP. Patch-type granuloma annulare: an institution-based study of 23 cases. J Cutan Pathol. 2020;47:785–93.

25. Blume-Peytavi U, Zouboulis CC, Jacobi H, et al. Successful outcome of cryosurgery in patients with granuloma annulare. Br J Dermatol. 1994;130:494–7.

26. COMSOL. COMSOL Multiphysics version 5.4. Acoustics module. User's guide and model library. COMSOL; 2018.

27. Andreozzi A, Brunese L, Iasiello M, et al. Modeling heat transfer in tumors: a review of thermal therapies. Ann Biomed Eng. 2019;47:676–93.

28. Liu X, Xue R, Ruan Y, et al. Effects of injection pressure difference on droplet size distribution and spray cone angle in spray cooling of liquid nitrogen. Cryogenics. 2017;83:57–63.

29. Goss SA, Frizzell LA, Dunn F. Ultrasonic absorption and attenuation in mammalian tissues. Ultrasound Med Biol. 1979;5:181–6.

30. van Rhoon GC. Is CEM43 still a relevant thermal dose parameter for hyperthermia treatment monitoring? Int J Hyperthermia. 2016;32:50–62.

31. Zhmakin AI. Physical aspects of cryobiology. Phys-Usp. 2008;51:231.

32. Kumari T, Kumar D, Rai KN, et al. Numerical solution of DPL heat transfer model in multi-layer biological skin tissue of the living body during hyperthermia treatment. Mech Based Des Struct Mach. 2023;51:159–78.

33. Choudhary B, Udayraj. Local and overall convective heat transfer coefficients for human body with air ventilation clothing: parametric study and correlations. Build Environ. 2023;229: 109953.

34. Tunnell JW, Torres JH, Anvari B. Methodology for estimation of time-dependent surface heat flux due to cryogen spray cooling. Ann Biomed Eng. 2002;30:19–33.

35. Sun F, Martínez-Suástegui L, Wang G-X, et al. Numerical prediction of the intracellular ICE formation zone during cryosurgery on a nodular basal cell carcinoma using liquid nitrogen spray. Int J Spray Combust Dyn. 2012;4:341–79.

36. Kumari C, Kumar A, Sarangi SK, et al. Effect of adjuvant on cutaneous cryotherapy. Heat Mass Transfer. 2019;55:247–60.

37. Soegaard S, Aarup V, Serup J, et al. High-frequency (20 MHz) high-intensity focused ultrasound system for dermal intervention: a 12-week local tolerance study in minipigs. Skin Res Technol. 2020;26:241–54.

38. Zawada T, Bove T. Strongly focused HIFU transducers with simultaneous optical observation for treatment of skin at 20 MHz. Ultrasound Med Biol. 2022;48:1309–27.

39. Calik J, Zawada T, Bove T. Treatment of condylomata acuminata using a new non-vapor-generating focused ultrasound method following imiquimod 5% cream. CDE. 2022;14:275–82.

40. Bachu VS, Kedda J, Suk I, et al. High-intensity focused ultrasound: a review of mechanisms and clinical applications. Ann Biomed Eng. 2021;49:1975–91.

41. Moran CM, Bush NL, Bamber JC. Ultrasonic propagation properties of excised human skin. Ultrasound Med Biol. 1995;21:1177–90.

42. Mortazavi S, Mokhtari-Dizaji M. Numerical study of high-intensity focused ultrasound (HIFU) in fat reduction. Skin Res Technol. 2023;29:e13280.

43. Nishimura S, Martin CJ, Jardine RJ, et al. A new approach for assessing geothermal response to climate change in permafrost regions. Géotechnique. 2009;59:213–27.

44. Nakagawa N, Matsumoto M, Sakai S. In vivo measurement of the water content in the dermis by confocal Raman spectroscopy. Skin Res Technol. 2010;16:137–41.